Iranian Journal of Materials Forming 12 (4) (2025) 34-43

Online ISSN: 2383-0042

IJMF

Iranian Journal of Materials Forming

Journal Homepage: http://ijmf.shirazu.ac.ir

Research Article

Microstructure and Mechanical Properties of Al-TiC Composite Fabricated by Accumulated Extrusion Bonding (AEB)

Ali Jafari and Nozar Anjabin*

Department of Materials Science and Engineering, School of Engineering, Shiraz University, Shiraz, Iran

ARTICLE INFO

Article history:

Received: 13 August 2025
Reviewed: 26 August 2025
Revised: 7 September 2025
Accepted: 17 September 2025

Keywords:

Aluminum composite
TiC
Accumulated extrusion bonding
Mechanical properties

Please cite this article as:

Jafari, A., & Anjabin, N. (2025). Microstructure and mechanical properties of Al-TiC composite fabricated by accumulated extrusion bonding (AEB). *Iranian Journal of Materials Forming*, *12*(4), 34-43. https://doi.org/10.22099/IJMF.2025.53979.1344

ABSTRACT

There is a growing demand for the use of light metals such as Al and its alloys in various industrial applications due to their high strength-to-weight ratio. Many studies were conducted to improve their properties by developing fine-grained structures and/or adding reinforcing particles. In this study, Al-TiC composite samples were fabricated using the accumulated extrusion bonding (AEB) method, which is a severe plastic deformation technique. The effects of TiC particle volume fraction and the number of extrusion passes on the microstructure and mechanical properties of the composites were investigated. The results indicated that the AEB of the pure Al sample at 390°C, with a 90% reduction in cross-sectional area, achieved proper interlayer bonding. Composite samples were fabricated by incorporating varying content of TiC particles (0.5, 1, and 2 vol.%) between the layers. It was found that the strength and hardness of the composite increased with the volume fraction of reinforcing particles. After four AEB passes, the composite containing 2 vol.% TiC exhibited a uniform particle distribution, resulting in an 83% increase in tensile strength and a 156% increase in hardness compared to the annealed sample.

1. Introduction

The use of light metals such as aluminum, magnesium, and titanium has received much attention in various industries, including automotive, aerospace, and defense, due to their characteristics such as good corrosion resistance and high strength to weight ratio [1]. However, increasing the strength of light metals has always been one of the main challenges in their use. The formation of a fine-grained structure and the addition of reinforcing particles are effective strategies for improving the mechanical properties of these metals, leading to increased strength, hardness, and wear resistance [2]. Aluminum matrix composites reinforced with ceramic particles, such as TiC, exhibit desirable properties including high strength and light weight while maintaining ductility, which makes them highly attractive for aerospace and automotive industries [3, 4]. For instance, Yonetken et al. [5] used powder metallurgy

* Corresponding author
E-mail address: anjabin@shirazu.ac.ir (N. Anjabin)
https://doi.org/10.22099/IJMF.2025.53979.1344

(cold pressing followed by sintering) to fabricate Al-TiC composites with varying TiC particle content (3-12 wt.%) and showed that the hardness increased with TiC content. Habba et al. [6] also investigated the effect of TiC particles (0-12 vol.%) on the mechanical properties of Al–TiC composite sheets fabricated by mechanical alloying followed by hot rolling. They found that adding 12 vol.% TiC significantly increased the density, hardness, and wear resistance. Huang et al. [7] showed that the use of a composite filler metal containing TiC particles during arc welding of 5083 aluminum alloy led to a uniform distribution of TiC particles in the joint area, with increasing particle content improving hardness, tensile strength, and corrosion resistance. Krishna et al. [8] applied the stir casting technique to produce aluminum 7075 matrix composites reinforced with TiC particles, and reported that increasing TiC content from 0 to 6 wt.% enhanced mechanical properties. Jafarian et al. [9] investigated the effect of TiC nanoparticles on the microstructure and mechanical properties of Al-TiC composites fabricated by accumulated roll bonding (ARB). After 7 ARB cycles, the grain size was reduced to 200 nm, with a uniform particle distribution, resulting in significant improvements in both yield strength and ultimate tensile strength. Wang et al. [10] employed the compo-casting method to fabricate Al/TiC composite bars. To enhance the mechanical properties and refine the microstructure of the cast samples, they applied warm accumulative press bonding (APB) as a supplementary technique. Their findings indicated that integrating compo-casting with APB resulted in a more uniform particle distribution and significantly improved mechanical performance.

Accumulated extrusion bonding (AEB) is a relatively new severe plastic deformation method offering advantages such as the ability to apply high strain and achieve considerable cross-sectional area reduction in a single pass, along with the potential for industrial-scale applications [11-13]. During extrusion, the samples are subjected to a stress state dominated by compression, which enhances workability, increases plastic deformation capacity, and consequently improves the interlayer bonding [13, 14]. Compared with ARB, extrusion enables a much larger plastic strain per pass, which benefits grain refinement and effectively promotes interface bonding [15]. For example, Muralidharan et al. [11] and Xiang et al. [15] demonstrated that applying the AEB to pure aluminum sheets produced very fine-grained structures with high hardness and strength. The AEB method has also been used to produce metal matrix composites, including layered composites of pure magnesium and aluminum alloys with ultrafine grains [16], as well as aluminum matrix composites reinforced with graphene nanosheets (GNSs) [17].

To the best of our knowledge, no study has been published on the production of Al-TiC composites using the AEB method. Therefore, this study aims to investigate the feasibility of manufacturing Al-TiC composites via AEB and to evaluate the effect of process parameters on their mechanical properties. Tensile and hardness tests, along with microscopic studies, were conducted to investigate the mechanical properties and microstructural characteristics of these composites.

2. Materials and Methods

2.1. Raw materials

A commercially pure aluminum sheet (chemical composition specified in Table 1) with a thickness of 5 mm in rolled form was used in the current study. Titanium carbide particles approximately 5 μm in size (Fig. 1) were employed as reinforcement.

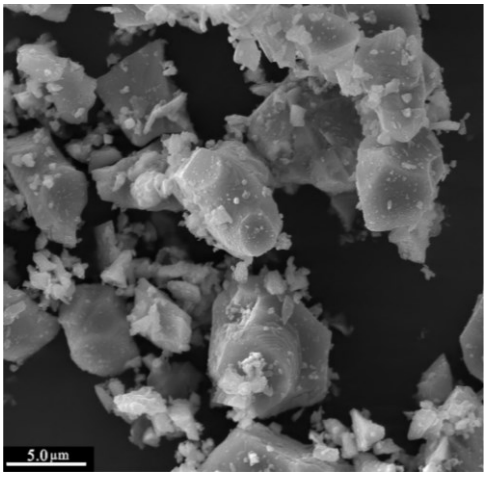

Fig. 1. SEM image of the TiC powder used in this study.

Table 1. Chemical composition of the aluminum used in this research

Elements	Al	Si	Fe	Ti	Zn
wt.%	99.585	0.027	0.352	0.02	0.016

2.2. AEB die design

The geometric specifications of the designed extrusion die and its 3D model, prepared using AutoCAD software, are shown in Fig. 2. The die components were manufactured from H13 tool steel, and the die angle was set to 45 degrees.

2.3. AEB process

To perform the AEB process, aluminum sheets with dimensions of 100 × 25 × 5 mm were cut from the as received annealed sheet. First, surface preparation was carried out and for composite samples, TiC particles were added. Then, the sheets were stacked and subjected to the extrusion process. Subsequently, the extruded sheet was re-cut, and after surface preparation and stacking, it was extruded again. This operation was repeated for up to four extrusion passes. The process is schematically illustrated in Fig. 3.

To enhance the bonding quality in the AEB process, and ensure the aluminum sheets were free of contamination, they were initially soaked in an acetone bath to eliminate grease. Following this, a rotating brush was used to remove any remaining impurities and surface oxides, leaving the sheets clean with a rough surface.

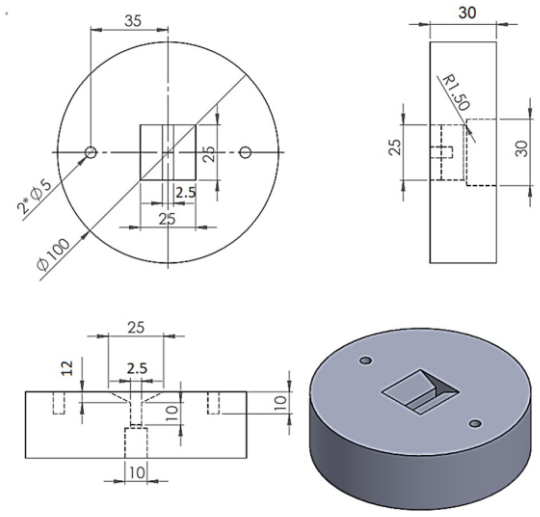

Fig. 2. Geometrical specifications of the extrusion die (dimensions are in millimeters).

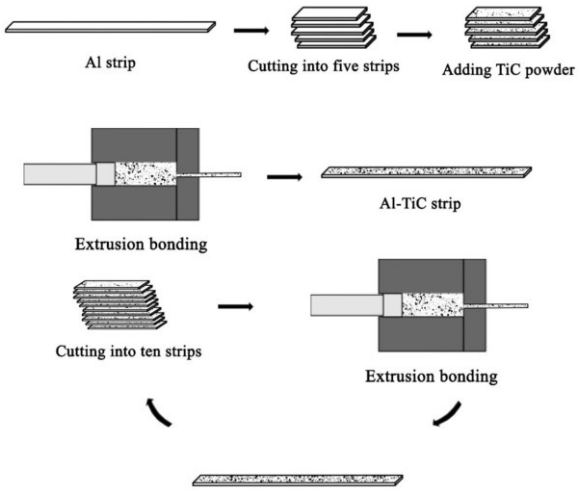

Fig. 3. Schematic of the accumulated extrusion bonding process for composites.

For the composite samples, after surface preparation of the sheets, TiC particles with different volume percentages (0.5, 1, and 2%) were uniformly distributed between the aluminum sheets. The sheets were then stacked and subjected to the extrusion process. To lubricate the contact surfaces between the die and the samples, Teflon and a lubricating fluid were applied. Additionally, to perform the high-temperature extrusion process, the sample and die assembly were preheated for 30 minutes in an elemental belt furnace. The extrusion process was carried out using a hydraulic press with a capacity of 20 tons, operating at a cross-head speed of 0.05 mm/s. The AEB process was successfully conducted at a temperature of 390 °C with a cross-sectional area reduction of 90% per pass, for up to 4 passes on both pure aluminum and Al-TiC composite samples. At the beginning of the extrusion process, five aluminum sheets, each with a thickness of 5 mm, were used. In subsequent passes, the extruded sheet was cut into ten sheets, which were then stacked for further extrusion. The number of layers after each process pass can be calculated using the formula $5 \times 10^{(n-1)}$, where n is the number of passes. Table 2 summarizes the specific conditions for each stage of the employed AEB process.

2.4. Evaluation of mechanical properties and microstructure

Tensile and hardness tests were conducted to assess the mechanical properties of the fabricated samples.

Table 2. Regime of the AEB process used in this study

Pass number	Number of layers	Thickness of each layer (mm)	Total reduction (%)
1	5	0.5	90
2	50	0.05	99
3	500	0.005	99.9
4	5000	0.0005	99.99

The uniaxial tensile test was carried out according to ASTM E8 standard, at room temperature, with a constant cross-head speed of 2 mm/s. Hardness was measured using the Vickers hardness test according to ASTM E92 standard. To examine the bond quality between the aluminum layers and the distribution of TiC particles within the aluminum matrix, transverse cross-sections of the extruded samples were prepared using standard metallographic procedures and analyzed using optical microscopy and scanning electron microscopy (SEM). Additionally, the fracture surfaces of the composite samples after the tensile test were examined using SEM. X-ray diffraction (XRD) analysis was performed to identify the phases present in the composite samples.

3. Results and Discussion

3.1. Influence of deformation temperature and degree of area reduction

Initially, the extrusion process was performed at room temperature with an 80% reduction in cross-sectional area per pass. However, as shown in Fig. 4, proper bonding between the sheets was not achieved. Furthermore, due to the limited capacity of the press (200 kN) and the high extrusion force, the extrusion process could not be completed.

To reduce the extrusion force, at a cross-sectional area reduction of 80% per pass, deformation temperature was raised to 390 °C. Although the extrusion was completed, proper bonding between the layers was not achieved. Further investigations showed that increasing the cross-sectional area reduction to 90% at a deformation temperature of 390 °C resulted in proper bonding between the aluminum layers, as shown in Fig. 5. Additionally, the force required for extrusion was significantly reduced, and the process was successfully carried out using a 20-ton press.

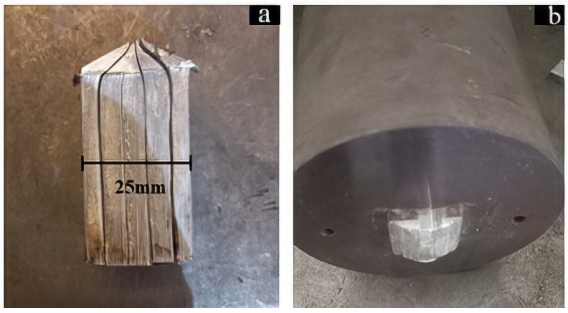

Fig. 4. Failed extrusion at room temperature.

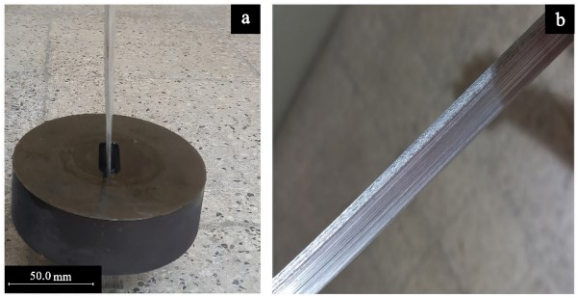

Fig. 5. AEB process with 90% cross-sectional area reduction at 390°C.

3.2. Microstructure

Fig. 6 shows optical microscopy images of composite samples with 2 vol.% TiC after different passes of the AEB process. From this figure, as the number of passes increased, the distribution of the powder in the Al matrix became more uniform, and the discontinuity observed between layers in the initial pass decreased. The uniform distribution of the powders in the transverse cross-section of the composite sample was further confirmed by the SEM image shown in Fig. 7. This uniform distribution of reinforcing particles in the aluminum matrix resulted in desirable mechanical properties in the composite.

3.3. Tensile properties

Fig. 8 presents the stress-strain curves of annealed pure aluminum and AEB-processed samples, including both pure aluminum and composite specimens containing varying percentages of TiC powder. Fig. 9 shows the corresponding yield strength, ultimate tensile strength, and elongation values derived from these stress-strain curves. The results indicate that applying four AEB passes increased both the yield strength and ultimate tensile strength of the pure aluminum sample compared to the annealed state, while reducing the elongation.

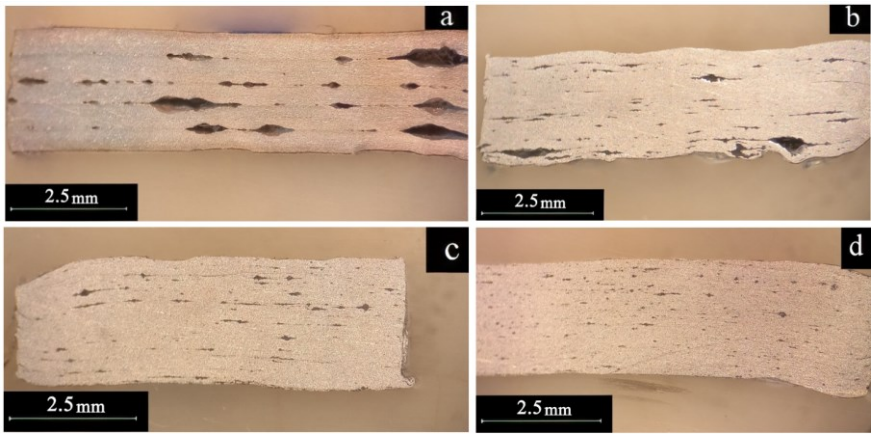

Fig. 6. Optical microscopy images of Al-2vol. %TiC samples after different AEB passes: (a) 1, (b) 2, (c) 3, and (d) 4 passes.

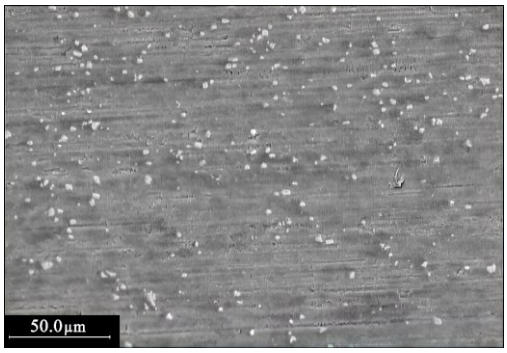

Fig. 7. SEM image of the Al-2 vol.%TiC sample subjected to 4 AEB passes, showing the uniform distribution of TiC particles.

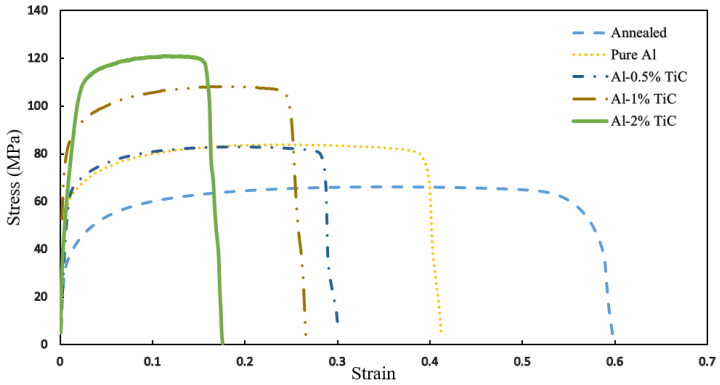

Fig. 8. Stress-strain curve of annealed pure aluminum, pure aluminum after AEB, and composite samples prepared by the AEB method.

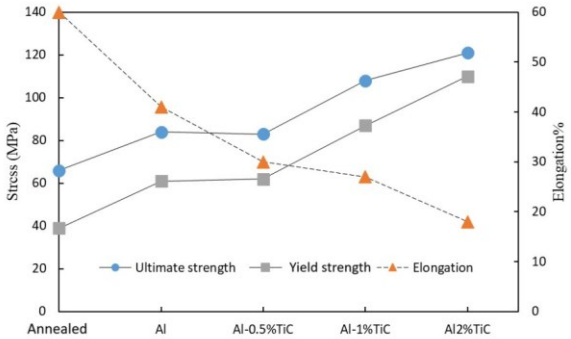

Fig. 9. Tensile strength, yield strength, and elongation of the annealed and AEB-processed samples with varying content of TiC.

The enhancement in strength can be attributed to dislocation strengthening and the formation of ultrafine grains (grain boundary strengthening) [9, 18]. Additionally, the incorporation of 0.5 vol.% TiC during the AEB process had no significant effect on yield strength or tensile strength, but it led to a reduction in elongation. However, increasing the amount of TiC powder in the extruded samples resulted in a notable improvement in both yield and tensile strength, accompanied by a further decrease in elongation.

Specifically, the addition of 2 vol.% TiC to pure Al resulted in an 83% increase in tensile strength and 170% increase in yield strength compared to the annealed sample.

Fig. 10 presents the hardness values for the annealed Al sample and those processed using the AEB method after four passes. The data indicate that the hardness of pure Al increased after four passes of AEB compared to the annealed condition. The hardness further increased when TiC particles were added, with higher volume fractions of these particles resulting in additional improvements in hardness. The strengthening effect of TiC particles in the composite is derived from three main mechanisms: load transfer from the metal matrix to the reinforcing particles [9, 19], strengthening due to dislocation-particle interactions, where small particles act as obstacles to dislocation motion during deformation [20], and the influence of the reinforcement on the matrix microstructure [19]. Reinforcement particles may accelerate the formation of ultrafine grains by inhibiting grain growth [9, 20]. Moreover, the increase in dislocation density due to the generation of geometrically necessary dislocations (GNDs) leads to enhanced composite strengthening. GNDs result from the deformation mismatch between secondary particles and the matrix during the forming process [9, 18, 19]. Additionally, temperature variations during the production process can generate GNDs to accommodate strain incompatibility arising from differences in the thermal expansion coefficients of the particles and the matrix [20].

Fig. 11 shows the stress-strain curves of the Al-2% TiC sample after applying different passes of the AEB process. The corresponding values of the tensile strength, yield strength, and elongation, derived from Fig. 11 are presented as a function of the number of AEB passes, in Fig. 12. According to these figures, increasing the number of passes to four, resulted in about a 36% increase in the tensile strength of the composite, while the elongation approximately doubled. From Fig. 12, the elongation of the composite sample decreased sharply after the first AEB pass compared to the annealed sample. This low ductility can be attributed to heavy strain hardening, uneven TiC particle distribution, and the presence of porosities, especially at the interface between the particles and the metal matrix after the first AEB pass. Additionally, insufficient bonding at the interface and the accumulation of particles between layers significantly reduced ductility in the initial passes [9, 18]. Increasing the number of AEB passes led to a more uniform distribution of TiC particles in the Al matrix, improved bonding between the layers, and the removal of most porosity in the layered structure, which enhanced strength and simultaneously improving ductility [18].

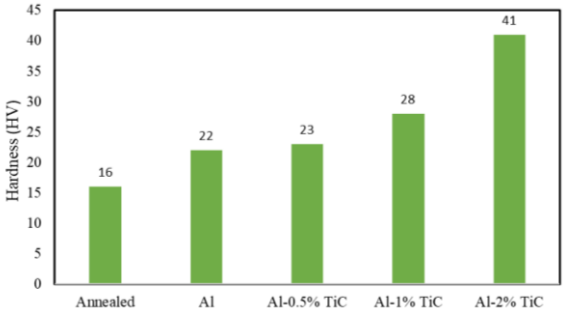

Fig. 10. Hardness values of the annealed Al sample and AEB-processed samples with varying content of TiC.

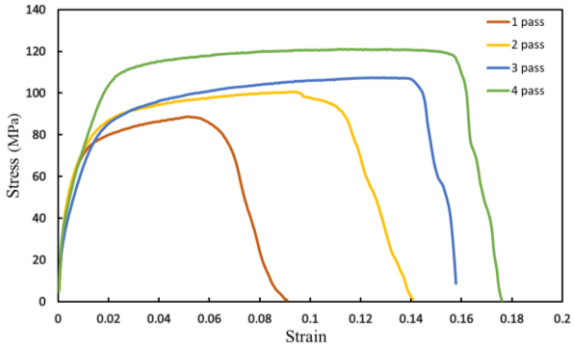

Fig. 11. Stress-strain curve of the Al-2%TiC sample after different passes of the AEB process.

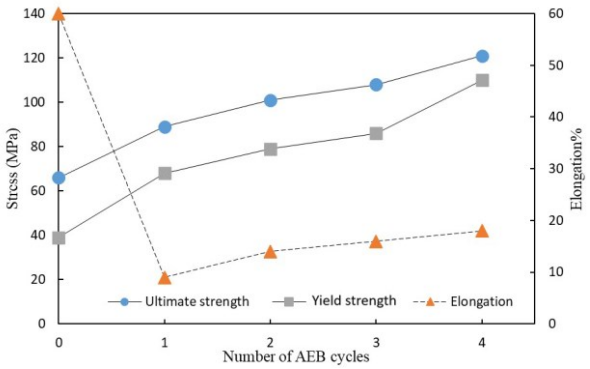

Fig. 12. Variation of tensile strength, yield strength, and elongation of the Al-2%TiC sample with the number of AEB process passes.

3.4. Fracture surface of tensile samples

SEM images of the fracture surface of the annealed pure Al and extruded samples containing different percentages of TiC (0 and 2 vol.%) after 4 AEB passes are shown in Fig. 13. According to these results, the fracture surface of the annealed pure Al sample shows deep and elongated dimples, indicating significant plastic deformation. In the extruded sample without powder, the number of dimples decreased; however, the presence of deep dimples still indicates a ductile fracture and considerable plastic deformation of the AEB-processed Al before fracture. When 2 vol.% TiC powder was added, the fracture surface structure changed noticeably, and both the depth and number of dimples were substantially reduced compared to the extruded pure Al sample. This indicates that adding TiC reduced the amount of plastic deformation of the material before fracture, leading to a more brittle fracture mode.

In Figs. 14 and 15, SEM images of the fracture surfaces of the composite samples containing 2% TiC powder are shown as a function of the AEB pass number. According to Fig. 14, as the number of passes increased, the bonding between the layers improved, and the discontinuity between them decreased. This contributed to an increase in accumulated plastic deformation. As shown in Fig. 15, increasing the number of passes reduced the formation of deep pores, causing the failure mode to shift toward brittle behavior. In this condition, the TiC particles acted as stress concentrators that initiated crack formation and led to failure. The results indicate that the shear-ductile mechanism remained significant in the failure of Al-TiC composites after several AEB passes; however, with increasing accumulated plastic deformation, the growth of pores became more limited and shallower, and fewer dimples were observed. Overall, as the number of passes increase, the TiC particle distribution became more uniform, and the fracture behavior of the composites tended to become more brittle.

3.5. X-ray diffraction pattern

Fig. 16 presents the XRD pattern of the Al-2 vol.% TiC sample, which confirms the presence of titanium carbide and alumina phases, along with aluminum, within the composite structure. During the AEB process, the high reactivity of aluminum with atmospheric oxygen led to the formation of a thin surface layer of aluminum oxide. Contaminants such as surface oxides on bonding surfaces acted as barriers that reduced bond quality. Therefore, grinding the sheet surface before bonding significantly improved bonding strength [21]. In the AEB process, similar to the ARB method, stacking layers during each pass introduced alumina particles into the Al bulk. This is reflected in the XRD pattern in Fig. 16 by distinct

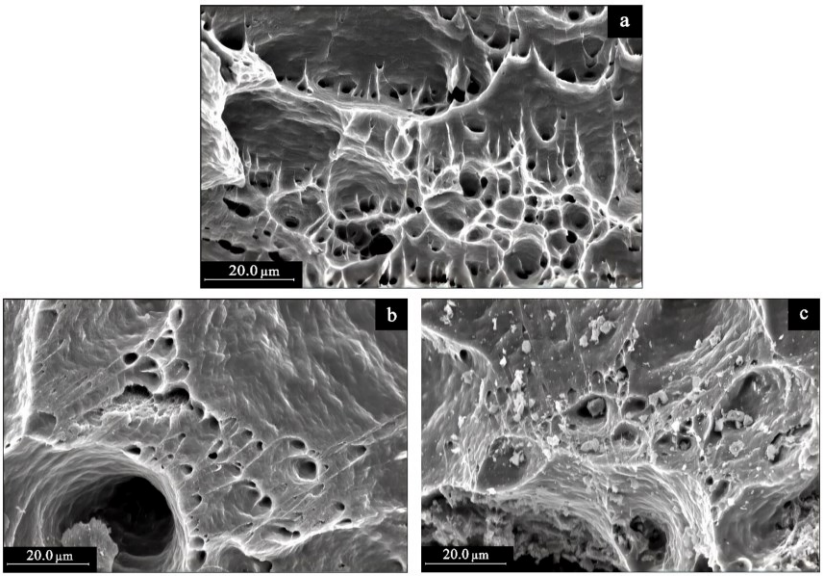

Fig. 13. SEM images of the fracture surfaces of (a) annealed pure Al, (b) pure Al after 4 AEB passes, and (c) Al-2%TiC sample after 4 AEB passes.

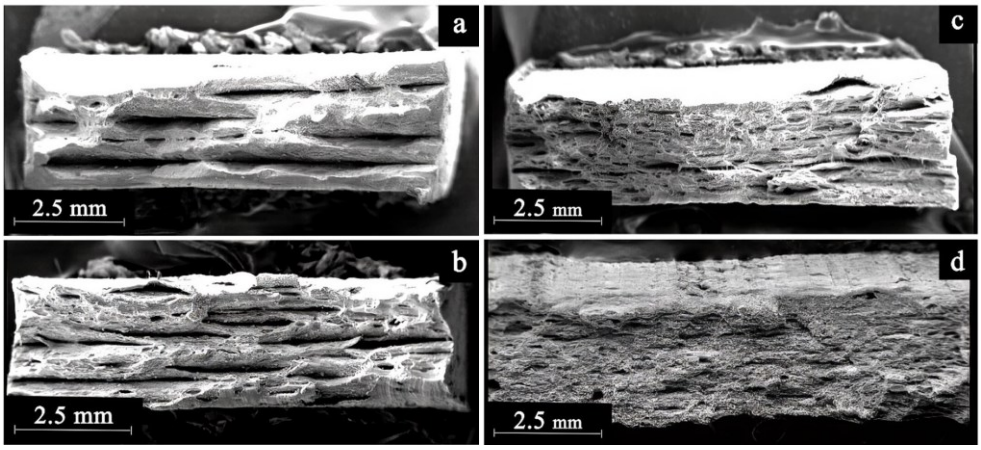

Fig. 14. SEM images of the fracture surfaces of Al-2%TiC samples, illustrating the evolution of interlayer bonding after being subjected to different numbers of AEB passes: (a) 1, (b) 2, (c) 3, and (d) 4 passes.

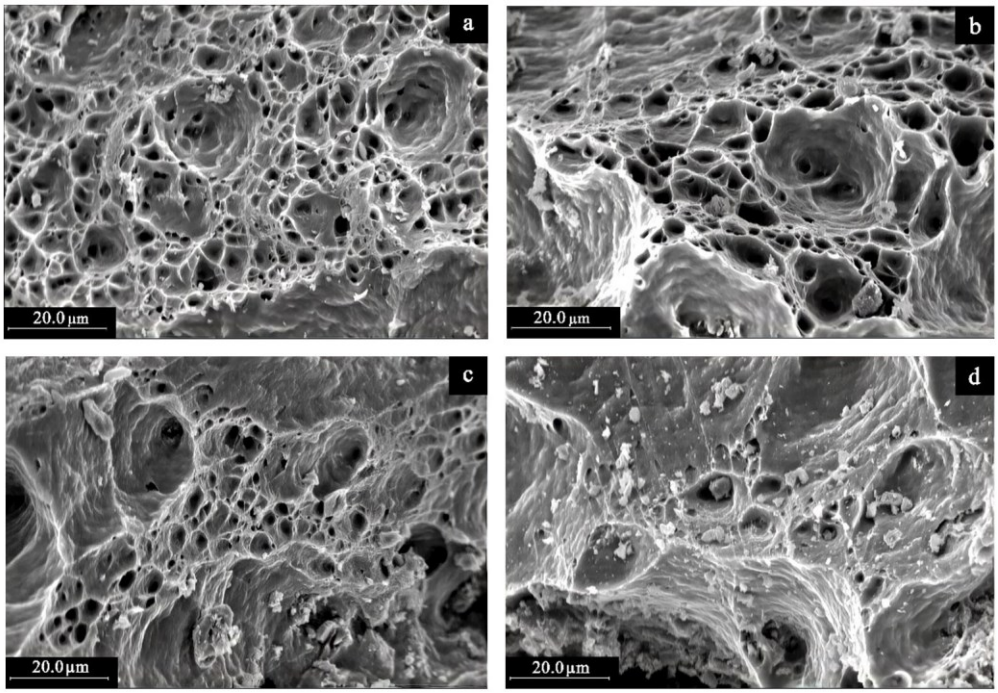

Fig. 15. SEM images of the fracture surfaces of Al-2%TiC samples at higher magnification after applying different numbers of AEB passes: (a) 1, (b) 2, (c) 3, and (d) 4 passes.

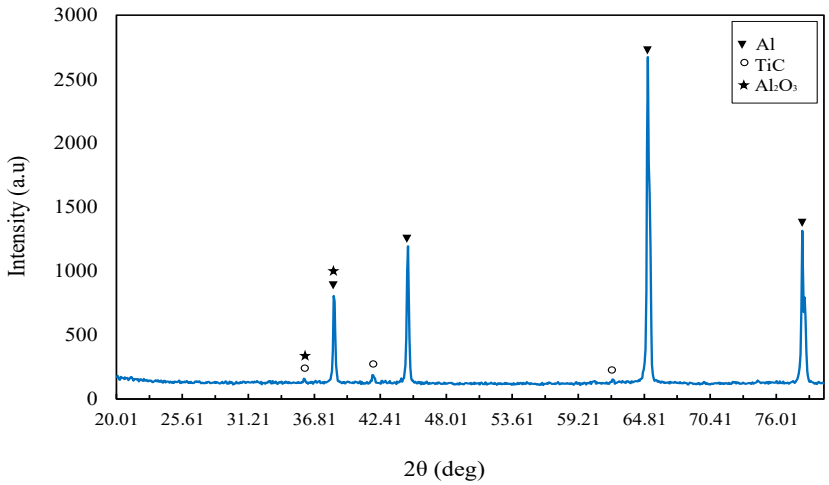

Fig. 16. X-ray diffraction pattern of the Al-2 vol.%TiC composite sample.

peaks corresponding to the Al_2O_3 phase. These oxide particles can inhibit grain boundary movement, thereby slowing down grain growth and altering the mechanical behavior [22].

4. Conclusions

In this study, the accumulated extrusion bonding method was employed to produce the Al-TiC composite, and the effects of parameters such as TiC powder volume fraction and the number of extrusion passes on the composite's properties were investigated. The extrusion process was successfully conducted using a 90% reduction in cross-sectional area per pass at 390 °C, resulting in proper bonding between the layers. Increasing the number of AEB passes to four led to a more uniform distribution of TiC particles within the Al matrix. The tensile strength increased from 66 MPa for the annealed sample to 121 MPa for the composite containing 2% TiC, and the hardness rose from 16 HV to 41 HV. Analysis of the fracture surfaces revealed that as both the number of passes and the TiC content increased, the depth and number of dimples on the fracture surface decreased, indicating a shift toward a more brittle fracture mode.

Authors' contributions

A. Jafari: Data curation, Formal analysis, Investigation, Methodology, Validation, Writing – original draft

N. Anjabin: Conceptualization, Formal analysis, Investigation, Supervision, Validation, Writing – review & editing

Conflict of interest

The authors declare that there is no conflict of interest.

Funding

The authors declare that no funds, grants, or other support were received.

5. References

[1] Li, C., & Feng, Q. (2023). Light alloys and their applications. *Metals*, *13*(3), 561-563. https://doi.org/10.3390/met13030561

[2] Ghalehbandi, S. M., Malaki, M., & Gupta, M. (2019). Accumulative roll bonding—a review. *Applied Sciences*, *9*(17), 3627-3638. https://doi.org/10.3390/app9173627

[3] Ravikumar, M., Reddappa, H., & Suresh, R. (2018). Aluminium composites fabrication technique and effect of improvement in their mechanical properties–A review. *Materials Today: Proceedings, 5*(11), 23796-23805. https://doi.org/10.1016/j.matpr.2018.10.171

[4] Oyewo, A. T., Oluwole, O. O., Ajide, O. O., Omoniyi, T.E., & Hussain, M. (2024). A summary of current advancements in hybrid composites based on aluminium matrix in aerospace applications. *Hybrid Advances*, *5*, 100117-100130. https://doi.org/10.1016/j.hybadv.2023.100117

[5] Yonetken, A., Çakmakkaya, M., & Oguz, Y. (2015). Production and characterization of Al-TiC composite materials, *Proceedings of the 1st International Conference on Engineering and Natural Sciences*, Macedonia.

[6] Habba, M. I., Barakat, W. S., Elnekhaily, S. A., & Hamid, F. (2024). Microstructure and tribological behavior of Al–TiC composite strips fabricated by a multi-step densification method. *Scientific Reports*, *14*(1), 20767-20787. https://doi.org/10.1038/s41598-024-70560-x

[7] Huang, Q., He, R., Wang, C., & Tang, X. (2019). Microstructure, corrosion and mechanical properties of TiC particles/Al-5Mg composite fillers for tungsten arc welding of 5083 aluminum alloy. *Materials*, *12*(18), 3029-3043. https://doi.org/10.3390/ma12183029

[8] Krishna Prasad, S., Dayanand, S., Rajesh, M., Nagaral, M., Auradi, V., & Selvaraj, R. (2022). Preparation and mechanical characterization of TiC particles reinforced Al7075 alloy composites. *Advances in Materials Science and Engineering*, (1), 7105189-7105199. https://doi.org/10.1155/2022/7105189

[9] Jafarian, H., Habibi-Livar, J., & Razavi, S.H. (2015). Microstructure evolution and mechanical properties in ultrafine grained Al/TiC composite fabricated by accumulative roll bonding. *Composites Part B: Engineering*, 77, 84-92. https://doi.org/10.1016/j.compositesb.2015.03.009

[10] Wang, W., Heydari Vini, M., & Daneshmand, S. (2022). Mechanical and wear properties of Al/TiC composites fabricated via combined compo-casting and APB process. *Crystals*, *12*(10), 1440-1450. https://doi.org/10.3390/cryst12101440

[11] Muralidharan, G. K., & Verlinden, B. (2016). Novel severe plastic deformation technique-accumulated extrusion (AccumEx). *Materials Science and Technology*, *32*(6), 547-555. https://doi.org/10.1179/1743284715Y.0000000121

[12] Han, T., Huang, G., Ma, L., Wang, G., Wang, L., & Pan, F. (2019). Evolution of microstructure and mechanical properties of AZ31 Mg alloy sheets processed by accumulated extrusion bonding with different relative orientation. *Journal of Alloys and Compounds*, *784*, 584-591. https://doi.org/10.1016/j.jallcom.2019.01.091

[13] Standley, M. R., & Knezevic, M. (2021). Towards manufacturing of ultrafine-laminated structures in metallic tubes by accumulative extrusion bonding. *Metals*, *11*(3), 389-413. https://doi.org/10.3390/met11030389

[14] Tekkaya, A., Groche, P., Kinsey, B., & Wang, Z. (2023). Stress superposition in metal forming. *CIRP annals*, *72*(2), 621-644. https://doi.org/10.1016/j.cirp.2023.04.090

[15] Xiang, C., Huang, G. S., & Jiang, B. (2019). Grain refinement and mechanical properties of pure aluminum processed by accumulative extrusion bonding. *Transactions of Nonferrous Metals Society of China*, *29*(3), 437-447. https://doi.org/10.1016/S1003-6326(19)64953-8

[16] Xin, Y., Hong, R., Feng, B., Yu, H., Wu, Y., & Liu, Q. (2015). Fabrication of Mg/AL multilayer plates using an accumulative extrusion bonding process. *Materials Science and Engineering: A*, *640*, 210-216. https://doi.org/10.1016/j.msea.2015.06.008

[17] Wu, G., Yu, Z., Jiang, L., Zhou, C., Deng, G., Deng, X., & Xiao, Y. (2019). A novel method for preparing graphene nanosheets/Al composites by accumulative extrusion-bonding process. *Carbon*, *152*, 932-945. https://doi.org/10.1016/j.carbon.2019.06.077

[18] Alizadeh, M., & Paydar, M. (2010). Fabrication of nanostructure Al/SiCP composite by *Materials Science and Technology* accumulative roll-bonding (ARB) process. *Journal of Alloys and Compounds*, *492*(1-2), 231-235. https://doi.org/10.1016/j.jallcom.2009.12.026

[19] Dai, L., Ling, Z., & Bai, Y. (2001). Size-dependent inelastic behavior of particle-reinforced metal–matrix composites. *Composites Science and Technology*, *61*(8), 1057-1063. https://doi.org/10.1016/S0266-3538(00)00235-9

[20] Rezayat, M., Akbarzadeh, A., & Owhadi, A. (2012). Production of high strength Al–Al2O3 composite by accumulative roll bonding, *Composites Part A: Applied Science and Manufacturing*, *43*(2), 261-267. https://doi.org/10.1016/j.compositesa.2011.10.015

[21] Trajano, A. A., Corrêa, E. C. S., Aguilar, M. T. P., & Cetlin, P. R. (2024). Accumulative roll bonding (ARB) and Cross accumulative roll bonding (CARB) in aluminum: A review. *Materials Science and Technology*, 02670836241303270. https://doi.org/10.1177/02670836241303270

[22] Kwan, C., Wang, Z., & Kang, S. B. (2008). Mechanical behavior and microstructural evolution upon annealing of the accumulative roll-bonding (ARB) processed Al alloy 1100, *Materials Science and Engineering: A*, *480*(1-2), 148-159. https://doi.org/10.1016/j.msea.2007.07.022